International Journal for Modern Trends in Science and Technology
Volume 12, Issue 04, pages 695-705.
ISSN: 2455-3778 online
Available online at: http://www.ijmtst.com/vol12issue04.html
DOI: https://doi.org/10.5281/zenodo.19536636

Solar Assisted EV Charging Microgrid with Bidirectional Inverter

Sk. Abdul Rahiman, G. Chaitanya Krishna, K. Meghana, Akash

Department of Electrical and Electronics Engineering, Vasireddy Venkatadri Institute of Technology, Pedakakani, Namburu, Guntur, India.

To Cite this Article
Sk. Abdul Rahiman, G. Chaitanya Krishna, K. Meghana & Akash (2026). Solar Assisted EV Charging Microgrid with Bidirectional Inverter. International Journal for Modern Trends in Science and Technology, 12(04), 695-705. https://doi.org/10.5281/zenodo.19536636

Article Info
Received: 16 March 2026; Revised: 06 April 2026; Accepted: 10 April 2026.

KEYWORDS

Electric Vehicle (EV) Charging, Bidirectional Inverter, Active Power Filter (APF), Photovoltaic (PV) System, Power Quality Improvement, Harmonic Mitigation, Energy Management System (EMS).

ABSTRACT

The rapid growth of electric vehicles (EVs) and the increasing demand for sustainable energy solutions have driven the need for advanced and efficient charging infrastructures. This paper presents the design and performance analysis of a solar-assisted EV charging microgrid integrated with a bidirectional inverter and active power filtering capability. The proposed system utilizes photovoltaic (PV) energy as a primary renewable source to support EV charging, thereby reducing dependence on conventional grid power and lowering carbon emissions. The bidirectional inverter facilitates two-way power flow between the EV, microgrid, and utility grid, enabling multiple modes of operation such as Grid-to-Vehicle (G2V), Vehicle-to-Grid (V2G), PV-to-Vehicle (PV2V), and PV-to-Grid (PV2G). In addition, hybrid operating modes including G2V+PV2V, V2G+PV2G, and PV2V+PV2G are implemented to enhance system flexibility under varying load and generation conditions. To address power quality issues arising from the integration of non-linear loads, the bidirectional inverter is further employed as an active power filter (APF). This functionality effectively mitigates harmonics, compensates reactive power, and improves the overall power quality at the point of common coupling (PCC). An intelligent control strategy ensures seamless mode transitions, optimal energy management, and stable system performance. The effectiveness of the proposed system is validated through extensive simulations carried out in MATLAB. Simulation results demonstrate efficient power flow control, enhanced utilization of solar energy, reduced harmonic distortion, and improved grid stability. The proposed system offers a reliable, flexible, and eco-friendly solution for next-generation EV charging and smart microgrid applications.

1. INTRODUCTION

The increasing global demand for energy, along with rising environmental concerns, has accelerated the transition toward renewable and sustainable energy sources [1]. Among these, solar photovoltaic (PV) systems have gained significant attention due to their clean, abundant, and eco-friendly characteristics [2]. In parallel, the rapid growth of electric vehicles (EVs) is transforming the transportation sector by reducing reliance on fossil fuels and lowering greenhouse gas emissions [3]. However, the large-scale adoption of EVs introduces challenges such as increased load demand, grid instability, and the need for efficient charging infrastructure [4]. Traditional EV charging stations mainly depend on the utility grid, which can result in peak load stress, voltage fluctuations, and higher energy costs [5]. To overcome these limitations, integrating renewable energy sources with EV charging systems has become an effective approach [6]. Solar-assisted EV charging microgrids offer a promising solution by utilizing locally generated solar energy, thereby reducing dependency on conventional power sources and improving system efficiency [7]. Furthermore, the incorporation of battery energy storage systems enhances reliability by compensating for the intermittent nature of solar power [8]. A key element in such systems is the bidirectional inverter, which enables two-way power flow between the EV, microgrid, and utility grid [9]. This feature allows multiple modes of operation, including Grid-to-Vehicle (G2V), Vehicle-to-Grid (V2G), PV-to-Vehicle (PV2V), and PV-to-Grid (PV2G) [10]. These operating modes provide flexibility in energy management and allow EVs to function not only as loads but also as distributed energy resources [11]. In V2G mode, EV batteries can supply power back to the grid during peak demand periods, improving grid stability and load balancing [12]. Similarly, PV2V and PV2G modes ensure efficient utilization of solar energy under varying environmental conditions [13]. Despite these advantages, the integration of power electronic converters and nonlinear loads in EV charging systems introduces power quality issues such as harmonics, reactive power imbalance, and voltage distortion at the point of common coupling (PCC) [14]. These issues can adversely affect the performance and reliability of the overall system [15]. To address these challenges, the bidirectional inverter can also operate as an active power filter (APF), mitigating harmonics and compensating reactive power [16]. This dual functionality significantly improves power quality and enhances system performance [17]. In addition, intelligent control strategies play a crucial role in ensuring efficient energy management and seamless transition between different operating modes [18]. Advanced control techniques enable optimal utilization of available resources, improve system stability, and enhance overall efficiency [19]. The integration of smart microgrid concepts further supports the coordination between renewable sources, storage systems, EVs, and the utility grid [20]. Recent research has focused on developing integrated systems that combine renewable energy generation, EV charging, and power quality improvement within a unified framework [21]. These systems aim to achieve higher efficiency, reliability, and sustainability while addressing the growing energy demands of modern power systems [22]. The use of MATLAB/Simulink-based modeling and simulation provides an effective platform for analyzing system performance under various operating conditions [23]. Simulation studies help in validating control strategies, evaluating power flow management, and assessing system stability [24]. Therefore, the development of a solar-assisted EV charging microgrid with a bidirectional inverter and active power filtering capability presents a comprehensive solution for next-generation energy systems [25]. This approach not only enhances renewable energy utilization but also improves grid performance, reduces environmental impact, and supports the sustainable growth of electric vehicle infrastructure.

II. SYSTEM CONFIGURATION

The proposed system consists of a solar-assisted EV charging microgrid integrated with a bidirectional inverter for efficient power flow management. A photovoltaic (PV) array is used as the primary energy source and is connected to a DC–DC boost converter controlled by an MPPT algorithm to extract maximum power under varying conditions. The output is fed to a

common DC link. A battery energy storage system is connected to the DC link through a bidirectional DC–DC converter, allowing energy storage during excess generation and supply during low PV output. The bidirectional inverter connects the DC side to the AC grid and enables two-way power flow between the grid, EV, and PV system. The system supports multiple operating modes such as Grid-to-Vehicle, Vehicle-to-Grid, PV-to-Vehicle, and PV-to-Grid, ensuring flexible energy utilization. Additionally, the inverter acts as an active power filter to reduce harmonics and improve power quality at the point of common coupling. An intelligent control strategy ensures proper coordination of all components, smooth operation, and stable performance under different operating conditions.

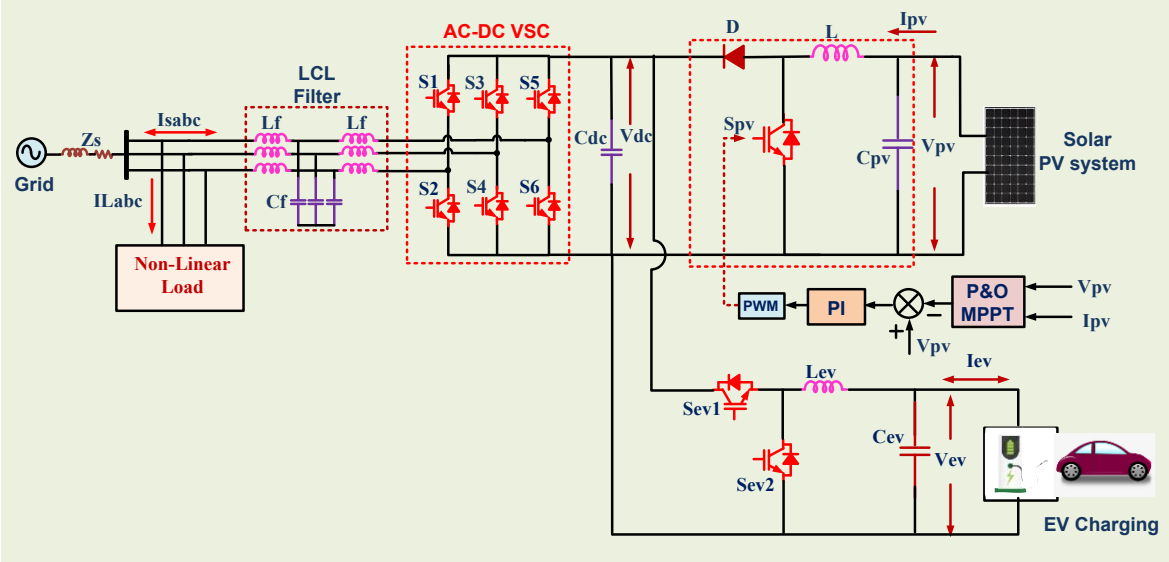

Fig.1 Proposed system Configuration

III. PROPOSED SYSTEM MODELING AND DESIGNING

A. Solar PV power generation system

The proposed grid-connected renewable energy setup includes a Solar Photovoltaic (PV) power generation system, which maximizes energy harvesting under varying solar irradiance and temperature conditions. The system uses a Maximum Power Point Tracking (MPPT) boost converter to regulate DC power extraction, enhancing overall system performance. The output is fed into a Voltage Source Inverter (VSI), which converts regulated DC voltage into AC for grid integration. The inverter operates with a high-frequency Pulse Width Modulation (PWM) technique to minimize switching losses and high power conversion efficiency. An LCL filter is incorporated to reduce total harmonic distortion (THD) and comply with grid standards. The solar PV system is integrated with a Battery Energy Storage System (BESS) through a bidirectional DC-DC converter to balance supply and demand. The power flow between the PV system, battery, and grid is managed through a coordinated energy management strategy.

a. Solar PV boost converter system configuration

The solar power system in a DC microgrid is crucial for efficient energy conversion and integration with other renewable energy sources. A perturb and observe (P&O) maximum power point tracking (MPPT) boost converter is used to optimize power extraction from the photovoltaic (PV) array, ensuring it operates at its maximum power point under varying solar irradiance conditions. The P&O MPPT algorithm continuously adjusts the operating point by introducing small perturbations to the duty cycle of the DC-DC boost converter. This architecture ensures stable power distribution for EV fast charging stations, minimizing power losses and improving overall efficiency. The DC microgrid benefits from this configuration by achieving improved renewable energy utilization, reduced reliance on grid power, and enhanced power quality. The bidirectional energy flow capability allows for effective integration with battery storage systems, ensuring energy availability even during low solar generation periods. Implementing this solar P&O MPPT boost converter allows the DC microgrid to manage power

distribution, support multiple EV chargers, and enhance sustainability by reducing carbon emissions through increased renewable energy penetration.

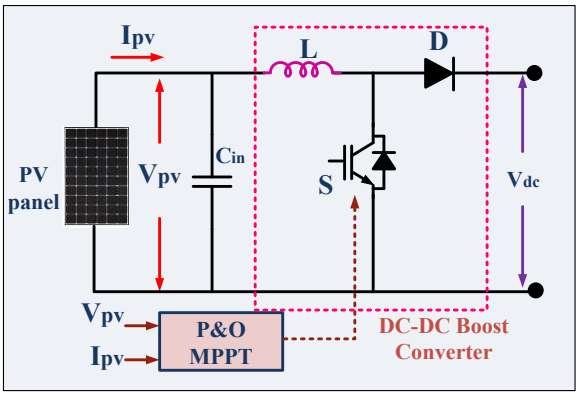

Fig. 2 solar PV P&O MPPT DC-DC boost converter

1. Single-Diode Solar PV Model: Designing a single-diode solar PV model involves analyzing the electrical characteristics of a photovoltaic (PV) cell. The single-diode model is one of the most commonly used to simulate the behavior of a PV cell. This model includes one diode, a current source, and series and shunt resistances to represent losses as shown in fig.5.
2. Basic Equation of the Single-Diode Model: The equation that governs the behavior of the single-diode PV model is derived from Kirchhoff's current law (KCL):

$$I = I_{Ph} - I_D - I_{sh} \quad (1)$$

Where: I = output current of the PV module (A), Iph = photocurrent, the current generated by light (A), ID = diode current (A), Ish = shunt current (A)

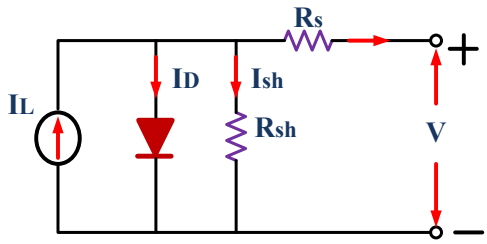

Fig. 3 equivalent model of PV solar.

3. Diode Current (ID): The current through the diode is described by the Shockley diode equation:

$$I_D = I_0\left(e^{\frac{V+IR_S}{nV_t}} - 1\right) \quad (2)$$

Where: I_0 = reverse saturation current of the diode (A), V = voltage across the PV cell (V), R_s = series resistance (Ω), n = diode ideality factor (typically between 1 and 2), V_t = thermal voltage (V), given by V_t=qkT

Here:

k = Boltzmann constant (1.38×10^{-23} J/K), T = temperature in Kelvin (K), q = electron charge (1.6×10^{-19} C)

4. Shunt Current (Ish): The current through the shunt resistance Rsh is modeled as:

$$I_{sh} = \frac{V+IR_s}{R_{sh}} \quad (3)$$

5. Equation of the Single-Diode PV Model: By substituting the expressions for ID and Ish into the main current equation, we get the complete form of the single-diode model:

$$I = I_{Ph} - I_0\left(e^{\frac{V+IR_S}{nV_t}} - 1\right) - \frac{V+IR_S}{R_{sh}} \quad (4)$$

6. Photocurrent I_{Ph}: The current generated by the cell due to light is proportional to the incident light and is affected by temperature. It can be modeled as:

$$I_{ph} = \left[I_{ph,ref} + \mu I_{Ph} \cdot (T - T_{ref})\right] \cdot \frac{G}{G_{ref}} \quad (5)$$

Where: $I_{ph,ref}$ = reference photocurrent at standard test conditions (STC), I_{Ph} = temperature coefficient of photocurrent (A/°C), T = cell temperature (°C), T_{ref} = reference temperature (usually 25°C), G = irradiance (W/m²), G_{ref} = reference irradiance at STC (1000 W/m²)

7. Saturation Current I_0: The reverse saturation current varies exponentially with temperature:

$$I_0 = I_{0,ref}\left(\frac{T}{T_{ref}}\right)^3 e^{\frac{Eg}{nV_t}\left(\frac{1}{T_{ref}} - \frac{1}{T}\right)} \quad (6)$$

Where:, $I_{0,ref}$ = reverse saturation current at reference temperature, Eg = bandgap energy of the semiconductor (typically 1.1 eV for silicon)

b. P&O MPPT Algorithm

The P&O MPPT algorithm adjusts the duty cycle (D) of the boost converter based on small perturbations to the PV voltage. The power change is determined as follows:

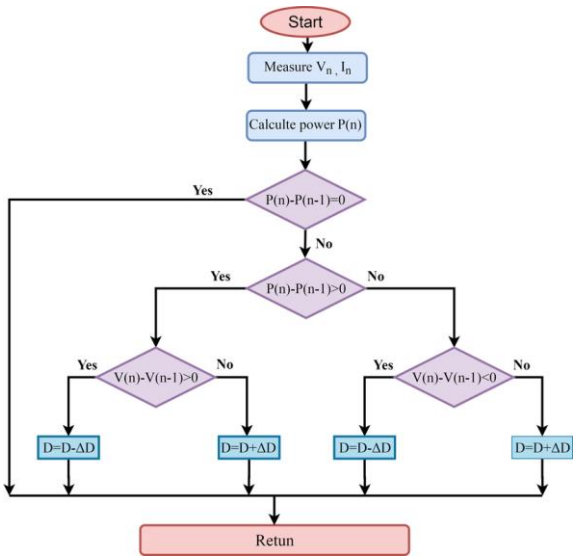

4. flow chart of P&O MPPT algorithm

$$\Delta P = P(k) - P(k-1) \quad (7)$$

$$\Delta V = V(k) - V(k-1) \quad (8)$$

$$if \Delta P > 0 \; and \; \Delta V > 0, increase \; V_{Pv} \quad (9)$$

$$if \Delta P < 0 and \Delta V > 0, decrease \; V_{Pv} \quad (10)$$

$$if \Delta P > 0 and \Delta V < 0, decrease \; V_{Pv} \quad (11)$$

$$if \Delta P < 0 and \Delta V < 0, increase \; V_{Pv} \quad (12)$$

The updated duty cycle is calculated as:

$$D(k+1) = D(k) + \alpha \cdot sign(\Delta P) \quad (13)$$

Where α is the step size for duty cycle adjustment.

c. Bidirectional Buck-Boost Converter for EV Charging in DC Microgrid

The bidirectional buck-boost converter plays a crucial role in managing energy flow between the battery energy storage system (BESS) and the DC bus in a microgrid. This converter enables both charging and discharging of the battery, ensuring stable power delivery for electric vehicle (EV) charging. In buck mode, the converter steps down the DC bus voltage to charge the battery, while in boost mode, it steps up the battery voltage to supply power to the microgrid or EV load. The control strategy dynamically adjusts the duty cycle to regulate power flow efficiently. The converter also helps stabilize the DC bus voltage, mitigating fluctuations from intermittent renewable energy sources like solar and wind. The energy management strategy ensures optimal charging and discharging cycles, enhancing battery lifespan and overall system efficiency.

1. Buck Mode (Battery Charging)

Output Voltage in Buck Mode:

$$V_b = D \cdot V_{dc} \quad (14)$$

Where: Vb = Battery voltage, Vdc = DC bus voltage, D = Duty cycle (0<D<1)

Inductor Current Ripple in Buck Mode:

$$\Delta I_L = \frac{(1-D)V_{dc}}{Lf_S} \quad (15)$$

Where: ΔIL = Inductor current ripple, L = Inductor value, fs = Switching frequency

2. Boost Mode (Battery Discharging)

Output Voltage in Boost Mode:

$$V_{dC} = \frac{V_b}{1-D} \quad (16)$$

Inductor Current Ripple in Boost Mode:

$$V_{dC} = \frac{V_b}{1-D} \quad (17)$$

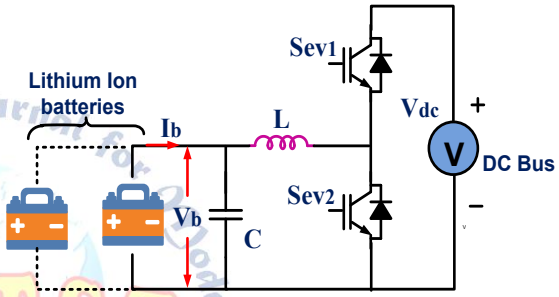

Fig.5 principle operation bidirectional dc-dc buck boost converter

d. Double-Loop Controller for EV Charging System

The control strategy for electric vehicle (EV) charging involves a double-loop control system to ensure efficient, stable, and safe charging. The outer voltage loop maintains a constant DC bus voltage, while the inner current loop regulates the battery charging current. A Proportional-Integral (PI) controller is used in both loops to minimize steady-state error and improve dynamic performance.

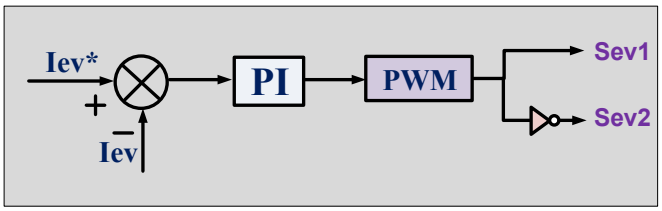

Fig. 6 double loop ev charging controller

1. Outer Voltage Loop: DC Bus Voltage Control

The outer voltage loop ensures the DC bus voltage (Vdc) remains stable and within the desired range. Since variations in EV charging loads and grid fluctuations

affect the DC bus voltage, this loop provides a reference current (Iev∗) for the inner current loop.

Error Signal Calculation:

$$e_v(t) = V_{dc}^* - V_{dC} \quad (18)$$

PI Controller Output (Reference EV Charging Current (I_{ev}^*)

$$I_{ev}^*(t) = K_{Pv}e_v(t) + k_{iv}\int e_v(t)\,dt \quad (19)$$

Where: I_{ev}^* = Reference charging current for the inner loop, Kpv= Proportional gain of voltage controller, Kiv= Integral gain of voltage controller

This reference current is then passed to the inner current loop for precise battery charging control.

2. Inner Current Loop: Battery Current Control

The inner current loop ensures the EV battery is charged with a smooth and regulated current to prevent over current issues and battery degradation. The PI controller in this loop generates the duty cycle for the DC-DC converter (buck or boost).

Error Signal Calculation:

$$e_i(t) = I_{ev}^* - I_{ev} \quad (20)$$

PI Controller Output (Duty Cycle Control)

$$D(t) = K_{Pi}e_i(t) + k_{ii}\int e_i(t)\,dt \quad (21)$$

Where: D = Duty cycle of the DC-DC converter, K_{Pi} = Proportional gain of current controller, k_{ii}= Integral gain of current controller

This duty cycle (D) is applied to the DC-DC converter, adjusting the output voltage and current to regulate battery charging.

IV. Modeling and Design of a Grid-Connected Voltage Source Converter (VSC) Controller

A bidirectional AC–DC voltage source converter (VSC) plays a crucial role in integrating renewable energy systems, electric vehicle charging stations, and microgrids by enabling efficient power exchange between the grid and the DC link. The converter is typically controlled using a synchronous reference frame (SRF)-based *d–q current control strategy*, which allows independent regulation of active and reactive power while maintaining DC-link voltage stability. This control approach ensures accurate tracking of reference currents and provides fast dynamic response under varying operating conditions. In addition to its primary function of power conversion, the proposed VSC is designed to operate as an active power filter (APF). In this mode, the converter compensates for harmonics generated by non-linear loads by injecting appropriate counteracting currents into the grid. The reference current generation is modified to include harmonic and reactive power components, enabling the VSC to mitigate current distortion and improve the power factor at the point of common coupling (PCC). The d-axis current component is typically used to regulate DC-link voltage and active power flow, while the q-axis component is utilized for reactive power compensation and harmonic mitigation. The integration of APF functionality within the VSC enhances overall system performance by reducing total harmonic distortion (THD), compensating reactive power, and improving grid current quality without requiring additional filtering hardware. This dual functionality makes the converter highly suitable for modern grid-connected applications, where both efficient energy transfer and high power quality are essential.

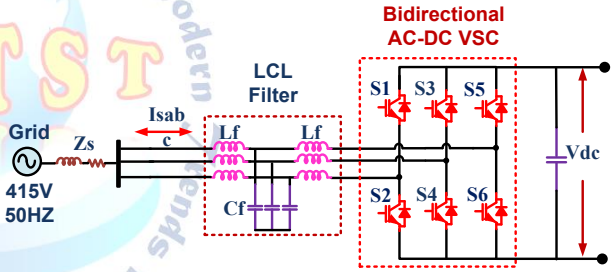

Fig.7 designing of bidirectional AC–DC voltage source converter

Initially, the DC-link voltage Vdc is sensed and compared with a reference value Vdcref. The resulting error signal is expressed as:

$$e(t) = V_{dc}^{ref} - V_{dc} \quad (22)$$

This error is processed through a proportional-integral (PI) controller to generate the reference direct-axis current id∗, which controls the active power exchange required to maintain a stable DC-link voltage:

$$i_d^*(t) = K_p e(t) + K_i\int e(t)dt \quad (23)$$

where Kp and Ki represent the proportional and integral gains of the controller.

At the same time, the three-phase grid/load currents (ia ,ib,ic) are measured and transformed into the synchronous rotating reference frame using Park's transformation. The transformation angle θ is obtained

from a three-phase phase-locked loop (PLL), which ensures synchronization with the grid voltage. The transformation is given by:

$$\begin{bmatrix} i_d \\ i_q \end{bmatrix} = \frac{2}{3}\begin{bmatrix} \cos\theta & \cos\left(\theta - \frac{2\pi}{3}\right) & \cos\left(\theta + \frac{2\pi}{3}\right) \\ -\sin\theta & -\sin\left(\theta - \frac{2\pi}{3}\right) & -\sin\left(\theta + \frac{2\pi}{3}\right) \end{bmatrix}\begin{bmatrix} i_a \\ i_b \\ i_c \end{bmatrix} \quad (24)$$

In the dq reference frame, the fundamental components of the current become DC quantities, while harmonic components appear as oscillatory signals. To isolate these harmonic components, filtering blocks (LPF/HPF) are used. The filtered outputs represent the fundamental or harmonic components depending on the filter design.

For unity power factor operation, the reference quadrature-axis current is set to:

$$i_q^* = 0 \quad (25)$$

The actual dq currents are then compared with their reference values to generate compensating current components:

$$i_d^{Comp} = i_d^* - i_d \quad (26)$$

$$i_q^{Comp} = i_q^* - i_q \quad (27)$$

These compensating signals are passed through a multiplexer (Mux) and then transformed back into the three-phase stationary frame using inverse Park transformation:

$$\begin{bmatrix} i_a^* \\ i_b^* \\ i_c^* \end{bmatrix} = \begin{bmatrix} \cos(\theta) & -\sin\theta \\ \cos\left(\theta - \frac{2\pi}{3}\right) & -\sin\left(\theta - \frac{2\pi}{3}\right) \\ \cos\left(\theta + \frac{2\pi}{3}\right) & -\sin\left(\theta + \frac{2\pi}{3}\right) \end{bmatrix}\begin{bmatrix} i_d^{Comp} \\ i_q^{Comp} \end{bmatrix} \quad (28)$$

The generated reference currents (ia∗,ib∗,ic∗) represent the desired compensating currents that the inverter must inject into the system to cancel harmonics and regulate power. These reference currents are compared with the actual inverter currents (iabc), and the error is fed into a hysteresis current controller. The hysteresis controller operates within a predefined band hhh and generates switching signals based on the current error:

$$i_{error} = i_{abc}^* - i_{abc} \quad (29)$$

Switching logic:

- If ierror>+h → upper switch OFF, lower switch ON
- If –h → upper switch ON, lower switch OFF

This results in fast dynamic response and precise tracking of reference currents.

Finally, the hysteresis controller generates six PWM gate signals (PWM1–PWM6) corresponding to the six switches of the three-phase voltage source converter (VSC). These switching signals ensure:

- DC-link voltage regulation
- Active power control (through id)
- Reactive power compensation (through iq)
- Harmonic elimination (APF operation)

Thus, the controller enables the bidirectional inverter to simultaneously perform energy exchange and power quality improvement, making it suitable for solar-assisted EV charging microgrid applications with non-linear loads.

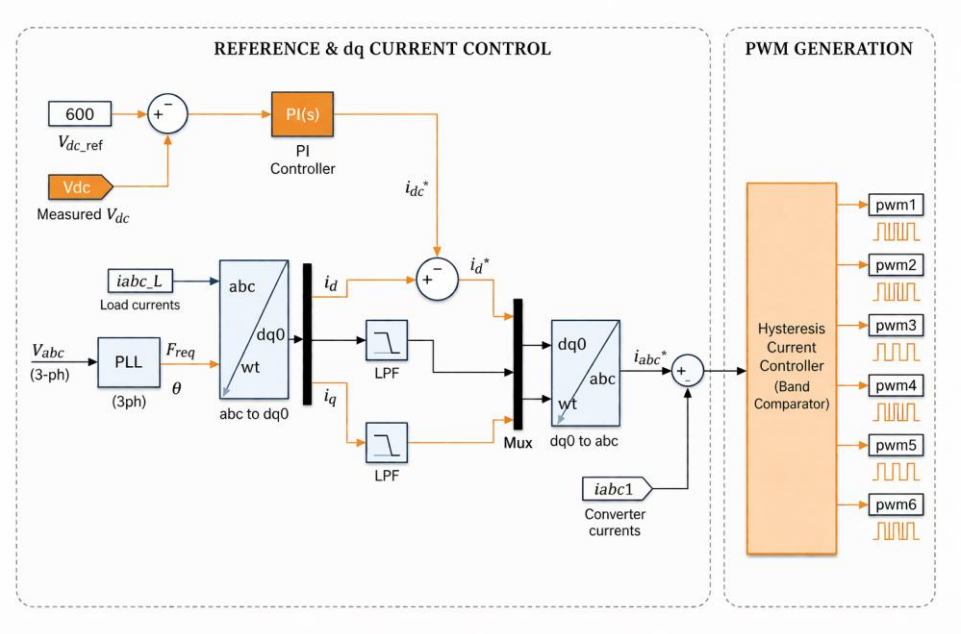

Figure 8: Designing of Reference dq current Controller for active power filter converter

V. SIMULATION RESULTS AND DISCUSSION

A. System Behavior under Varying Load and Generation Conditions

The simulation results demonstrate stable and coordinated operation of the grid, photovoltaic (PV) system, electric vehicle (EV), and load under varying conditions. The grid voltage remains balanced and sinusoidal at approximately ±200 V throughout the entire duration, indicating a strong and stable grid connection. In contrast, the grid current varies significantly over time, reflecting changes in power demand and generation. Initially, the current is moderate, then decreases, and later increases to a peak before reducing again after 1 second. This variation confirms that the inverter effectively controls current injection to regulate power flow while maintaining synchronization with the grid. The load voltage also remains constant and sinusoidal, showing that the system successfully maintains a stable supply to the load regardless of disturbances or changes in operating conditions. The load current appears consistent with minor variations, indicating that the load demand is relatively steady. This stability suggests that the control strategy ensures uninterrupted power delivery to the load, even when other components in the system are dynamically changing. The PV system exhibits a relatively stable voltage around 280–300 V, with a small dip observed around 0.4 seconds, likely due to a transient or change in operating conditions. The PV current, however, shows step changes, decreasing significantly around 0.4 seconds and then increasing again after 1 second. This behavior indicates that the PV system is operating under varying irradiance or control conditions, and the system is The EV characteristics reveal that the battery voltage gradually increases over time, while the current transitions from near zero to negative values, indicating a shift from idle or light operation to active charging. The increasing state of charge (SOC) further confirms that the EV is absorbing energy during the later stages of the simulation. This demonstrates proper bidirectional energy flow capability and effective EV charging control. The DC-link voltage remains relatively stable around 600 V, with some transient dips and overshoots corresponding to sudden changes in PV output and load or EV demand. Despite these disturbances, the DC-link quickly stabilizes, indicating effective DC-link voltage regulation and robust control performance. Finally, the power profiles show clear energy management among the system components. The load power remains nearly constant, while PV power varies in steps, and EV power becomes negative during charging periods. The grid power adjusts dynamically to balance the system, supplying power when PV generation is low and absorbing or reducing supply when PV generation is high. This confirms that the system successfully maintains power balance and demonstrates efficient integration of renewable energy and EV charging within a grid-connected framework.

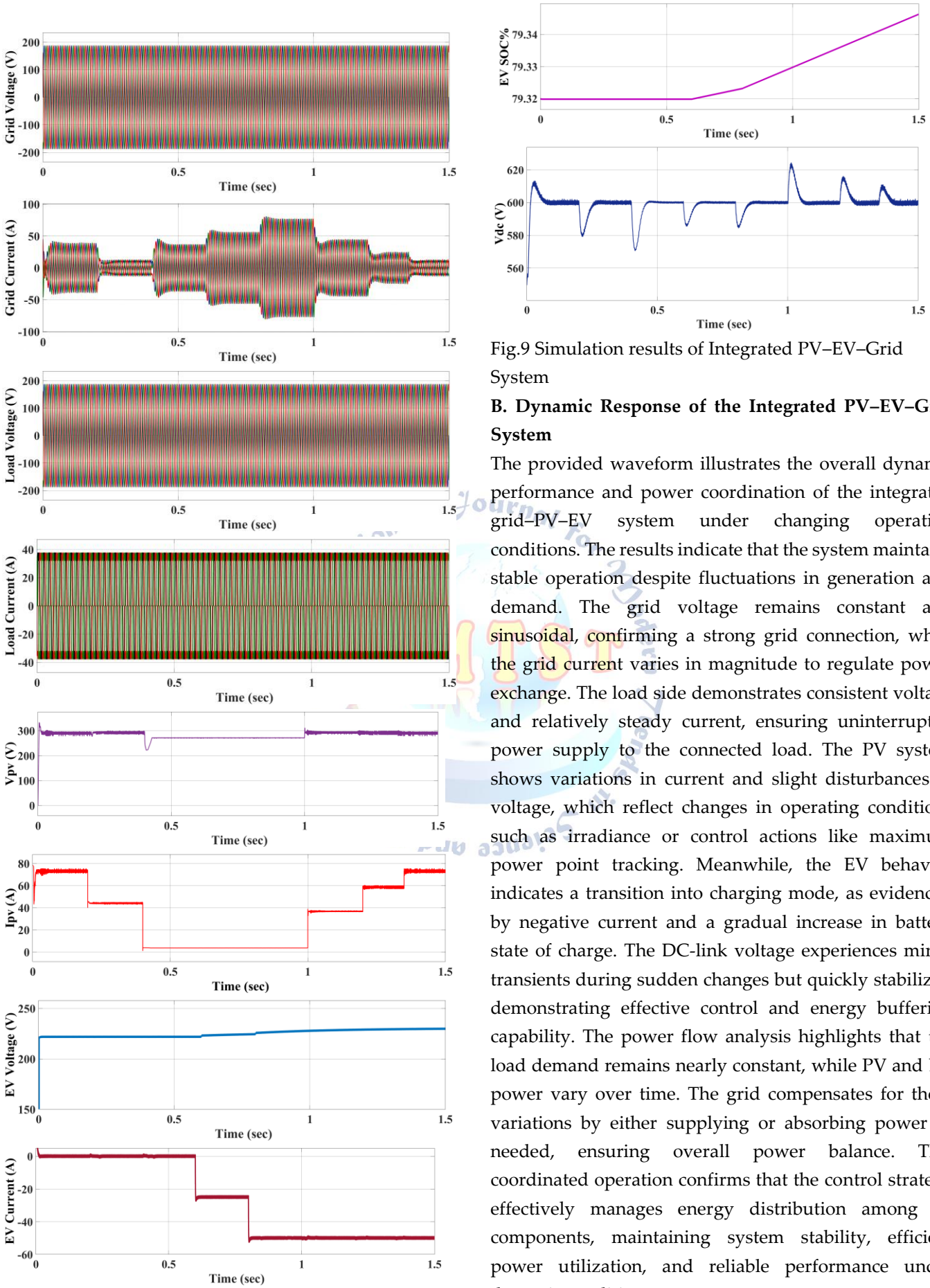

Fig.9 Simulation results of Integrated PV–EV–Grid System

B. Dynamic Response of the Integrated PV–EV–Grid System

The provided waveform illustrates the overall dynamic performance and power coordination of the integrated grid–PV–EV system under changing operating conditions. The results indicate that the system maintains stable operation despite fluctuations in generation and demand. The grid voltage remains constant and sinusoidal, confirming a strong grid connection, while the grid current varies in magnitude to regulate power exchange. The load side demonstrates consistent voltage and relatively steady current, ensuring uninterrupted power supply to the connected load. The PV system shows variations in current and slight disturbances in voltage, which reflect changes in operating conditions such as irradiance or control actions like maximum power point tracking. Meanwhile, the EV behavior indicates a transition into charging mode, as evidenced by negative current and a gradual increase in battery state of charge. The DC-link voltage experiences minor transients during sudden changes but quickly stabilizes, demonstrating effective control and energy buffering capability. The power flow analysis highlights that the load demand remains nearly constant, while PV and EV power vary over time. The grid compensates for these variations by either supplying or absorbing power as needed, ensuring overall power balance. This coordinated operation confirms that the control strategy effectively manages energy distribution among all components, maintaining system stability, efficient power utilization, and reliable performance under dynamic conditions.

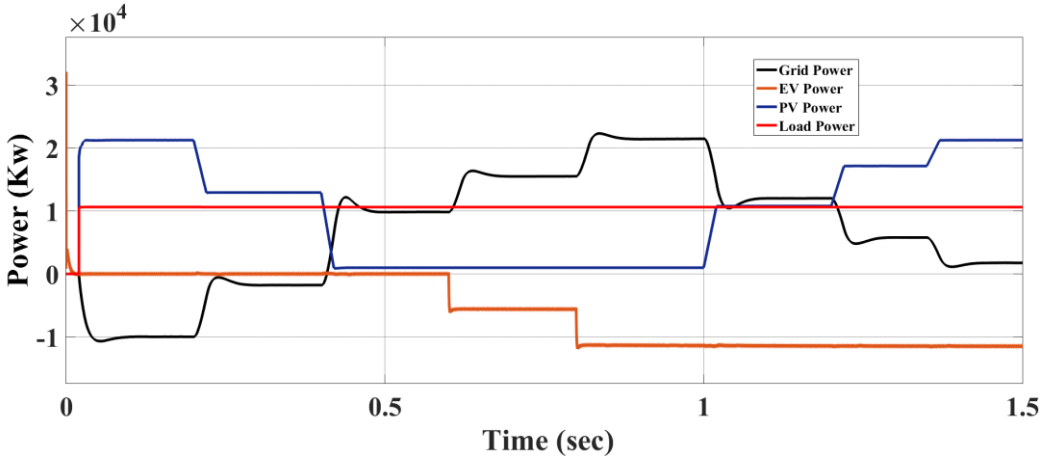

Fig. 10 Simulation result of Power Flow Coordination and System Stability

VI. CONCLUSION

This paper presented a solar-assisted EV charging microgrid integrated with a bidirectional inverter capable of both power flow management and active power filtering. The proposed system effectively utilizes photovoltaic (PV) energy to support EV charging, thereby reducing reliance on the utility grid and promoting sustainable energy usage. The bidirectional inverter enables flexible operation through multiple modes, including G2V, V2G, PV2V, and PV2G, as well as hybrid combinations, ensuring adaptability under varying generation and load conditions. The simulation results confirm that the system maintains stable voltage profiles, efficient current control, and balanced power flow across all operating modes. The EV charging and discharging processes are well-coordinated, with smooth transitions between modes and effective state-of-charge management. Additionally, the integration of active power filtering functionality significantly improves power quality by reducing harmonics and compensating reactive power at the point of common coupling. Overall, the proposed microgrid demonstrates reliable performance, enhanced solar energy utilization, and improved grid interaction. It provides a flexible and eco-friendly solution for modern EV charging infrastructure, contributing to reduced carbon emissions and supporting the development of smart and sustainable power systems. Future work may focus on hardware implementation, real-time control validation, and the integration of advanced energy management techniques such as artificial intelligence for further optimization.

Conflict of interest statement

Authors declare that they do not have any conflict of interest.

REFERENCES

[1] M. Ehsani, K. V. Singh, H. O. Bansal, and R. T. Mehrjardi, "State of the art and trends in electric and hybrid electric vehicles," IEEE Proc., vol. 109, no. 6, pp. 967–984, Jun. 2021.

[2] S. K. Rastogi, A. Sankar, K. Manglik, S. K. Mishra, and S. P. Mohanty, "Toward the vision of all-electric vehicles in a decade [energy and security]," IEEE Consum. Electron. Mag., vol. 8, no. 2, pp. 103–107, Mar. 2019.

[3] I. Hong, B. Kang, and S. Park, "Design and implementation of intelligent energy distribution management with photovoltaic system," IEEE Trans. Consum. Electron., vol. 58, no. 2, pp. 340–346, May 2012.

[4] Y.-M. Wi, J.-U. Lee, and S.-K. Joo, "Electric vehicle charging method for smart homes/buildings with a photovoltaic system," IEEE Trans. Consum. Electron., vol. 59, no. 2, pp. 323–328, May 2013.

[5] N. Kumar, V. Saxena, B. Singh, and B. K. Panigrahi, "Power quality improved grid-interfaced PV assisted onboard EV charging infrastructure for smart households consumers," IEEE Trans. Consum. Electron., vol. 69, no. 4, pp. 1091–1100, Nov. 2023.

[6] G. R. C. Mouli, P. Bauer, and M. Zeman, "System design for a solar powered electric vehicle charging station for workplaces," Appl. Energy, vol. 168, pp. 434–443, Apr. 2016.

[7] G. R. C. Mouli et al., "Economic and CO2 emission benefits of a solar powered electric vehicle charging station for workplaces in The Netherlands," in Proc. IEEE Transp. Electrific. Conf. Expo(ITEC), 2016, pp. 1–7.

[8] G. Carli and S. S. Williamson, "Technical considerations on power conversion for electric and plug-in hybrid electric vehicle battery charging in photovoltaic installations," IEEE Trans. Power Electron., vol. 28, no. 12, pp. 5784–5792, Dec. 2013.

[9] G. R. C. Mouli, P. Bauer, and M. Zeman, "Comparison of system architecture and converter topology for a solar powered electric vehicle charging station," in Proc. 9th Int. Conf. Power Electron (ECCE), 2015, pp. 1908–1915.

[10] V. M. Iyer, S. Gulur, and S. Bhattacharya, "Small-signal stability assessment and active stabilization of a bidirectional battery charger," IEEE Trans. Ind. Appl., vol. 55, no. 1, pp. 563–574, Jan./Feb. 2019.

[11] V. Monteiro, J. G. Pinto, and J. L. Afonso, "Experimental validation of a three-port integrated topology to interface electric vehicles and renewables with the electrical grid," IEEE Trans. Ind. Informat., vol. 14, no. 6, pp. 2364–2374, Jun. 2018.

[12] D. B. W. Abeywardana, P. Acuna, B. Hredzak, R. P. Aguilera, and V. G. Agelidis, "Single-phase boost inverter-based electric vehicle charger with integrated vehicle to grid reactive power compensation," IEEE Trans. Power Electron., vol. 33, no. 4, pp. 3462–3471, Apr. 2018.

[13] R. K. Lenka, A. K. Panda, R. Patel, and J. M. Guerrero, "PV Integrated multifunctional off-board EV charger with improved grid power quality," IEEE Trans. Ind. Appl., vol. 58, no. 5, pp. 5520–5532, Sep./Oct. 2022.

[14] V. Jain, B. Singh, and Seema, "A grid connected PV array and battery energy storage interfaced EV charging station," IEEE Trans. Transp. Electrif., vol. 9, no. 3, pp. 3723–3730, Sep. 2023.

[15] Q. Sun, H. Xie, X. Liu, F. Niu, and C. Gan, "Multiport PVassisted electric-drive-reconstructed bidirectional charger with G2V and V2G/V2L functions for SRM drive-based EV application," IEEE J. Emerg. Sel. Topics Power Electron., vol. 11, no. 3, pp. 3398–3408, Jun. 2023.

[16] J. Sharma, C. K. Sundarabalan, C. Balasundar, S. N. Santhanam, and J. M. Guerrero, "Conjugate-gradient based control in a gridintegrated PV with 24/7 distortion-free charging for bidirectional EV charger," IEEE Trans. Ind. Informat., vol. 20, no. 4, pp. 5206–5216, Apr. 2024.

[17] A. K. Mishra and T. Kim, "An economical light plug-in electric vehicle (LPEV) with on-board single-stage battery charging system," IEEE Trans. Ind. Appl., vol. 59, no. 5, pp. 6568–6579, Sep./Oct. 2023.

[18] S. Kumar, T. Upadhyay, and O. H. Gupta, "Power quality improvement and signal conditioning of PV array and grid interfaced off-board charger for electric vehicles with V2G and G2V capabilities," Chin. J. Electr. Eng., vol. 9, no. 4, pp. 132–143, Dec. 2023.

[19] S. Ghosh and B. Singh, "A multiport charger for light electric vehicles with function of powering domestic appliances," IEEE Trans. Consum. Electron., vol. 70, no. 1, pp. 308–317, Feb. 2024.

[20] L. Wang, H. Wang, M. Fu, J. Liang, and Y. Liu, "A three-port energy router for grid-tied PV generation systems with optimized control methods," IEEE Trans. Power Electron., vol. 38, no. 1, pp. 1218–1231, Jan. 2023.

[21] X. Zhang, H. Liu, P. Wheeler, and F. Wu, "Research on power decoupling and parameter mismatch of three-port isolated resonant DC– DC converter applied switch-controlled capacitor," IEEE Trans. Ind. Electron., vol. 70, no. 8, pp. 8098–8107, Aug. 2023.

[22] V. Narayanan and B. Singh, "SOGI-FLL-WDCRC filter for seamless control of microgrid for optimal coordination of conventional and renewable energy resources," IEEE Trans. Ind. Appl., vol. 59, no. 4, pp. 4821–4834, Jul./Aug. 2023.

[23] C. L. Bhattar and M. A. Chaudhari, "Centralized energy management scheme for grid connected DC microgrid," IEEE Syst. J., vol. 17, no. 3, pp. 3741–3751, Sep. 2023.

[24] S. Kang, J. Noh, and J.-W. Park, "Active distribution management system based on smart inverter control of PV/ESS integrated system," IEEE Trans. Ind. Electron., vol. 69, no. 8, pp. 7994–8003, Aug. 2022.

[25] P. K. Sorte, K. P. Panda, and G. Panda, "Current reference control based MPPT and investigation of power management algorithm for grid-tied solar PV-battery system," IEEE Syst. J., vol. 16, no. 1, pp. 386–396, Mar. 2022.